CONSTRAINTS ON NEUTRINO MASSES WITH LYMAN-α FOREST POWER SPECTRUM

Ch. YÈCHE
CEA-Saclay, Irfu F-91191 Gif-sur-Yvette, France

We present constraints on neutrino masses in the case of the ΛCDMν and ΛWDM models, using the one-dimensional Lyα-forest power spectrum measured the Baryon Oscillation Spectroscopic Survey (BOSS) of the Sloan Digital Sky Survey (SDSS-III), complemented by Planck 2015 Cosmic Microwave Background (CMB) data. Fitting Lyα data alone leads to cosmological parameters in excellent agreement with the values derived independently from CMB data, except for a weak tension on the scalar index n_s. Combining BOSS Lyα with Planck CMB constrains the sum of neutrino masses to $\sum m_\nu < 0.12$ eV (95% C.L.) including all identified systematic uncertainties. In the case of ΛWDM model, we issue the tightest bounds to date on pure dark matter particles: $m_X \gtrsim 4.35\,\mathrm{keV}$ (95% C.L.) for early decoupled thermal relics and its corresponding bound for a non-resonantly produced right-handed neutrino $m_s \gtrsim 26.4\,\mathrm{keV}$ (95% C.L.).

1 Introduction

The flux power spectrum of the Lyman-α (Lyα) forest in quasar absorption spectra is a powerful tool to study clustering in the Universe, at redshifts $\sim 2-4$. Compared to a model derived from a set of dedicated hydrodynamical simulations, the Lyα-flux power spectrum can provide valuable information on the formation of structures and their evolution. Furthermore, by probing scales down to a few Mpc, the 1D flux power spectrum is also sensitive to neutrino masses through the suppression of power on small scales that neutrinos induce because they become non-relativistic at small redshift and they therefore free-stream during most of the history of structure formation. We here use the 1D Lyα flux power spectrum measured by [1] with the DR9 release of BOSS quasar data , and a grid of 36 hydrodynamical simulations having a resolution equivalent to 3×3072^3 particles in a $(100\ h^{-1}\ \mathrm{Mpc})^3$ box [2, 3], to constrain both cosmology and the sum of the neutrino masses $\sum m_\nu$.

Cosmic Microwave Background (CMB) can also constrain $\sum m_\nu$. In the standard thermal history of the Universe, massless neutrinos have a temperature corresponding to ~ 0.17 eV at the epoch of last scattering. This temperature sets the range of masses for which neutrinos start to have an appreciable effect on the CMB power spectrum to $\sum m_\nu > 3 \times 0.17 = 0.51$ eV. Below this mass, the neutrinos are still relativistic at recombination and have no impact on the

primary CMB anisotropies. The latest limit on $\sum m_\nu$ from CMB data alone is at the level of 0.7 eV [4].

Lyα data alone have sensitivity to $\sum m_\nu$ at the level of about 1 eV due to the fact that the scales probed by Lyα forests are in the region where the ratio of the power spectra for massive to massless neutrinos is quite flat. However, a tight constraint on $\sum m_\nu$ can be obtained by combining CMB data, which probe the initial power spectrum unaffected by $\sum m_\nu$, and Lyα data, which probe the suppressed power spectrum. Thus, Lyα measures the power spectrum level, defined by σ_8 and Ω_m, CMB provides the correlations between these parameters and $\sum m_\nu$, and the joint use of these two probes significantly improves the constraint on $\sum m_\nu$ compared to what either probe alone can achieve.

In the case of ΛWDM models, when traveling, massive particles can interfere with the gravitational collapse of structures. This manifests in a step-like suppression in the matter power spectrum at scales above $\sim 0.01(\mathrm{km/s})^{-1}$ for particles of a few keV. These particles have a free-streaming scale which falls below the Mpc range and within the region probed by the Lyα forests of distant high redshift quasars. Lyα forest data therefore provide again an ideal tool to study keV-range WDM and give constraints on the lower-bound mass of early decoupled thermal relics.

2 Data, Simulations and Methodology

As our large-scale structure probe, we use the 1D Lyα-flux power spectrum measurement [1] from the first release of BOSS quasar data. The data consist of a sample of 13 821 spectra selected from the larger sample of about 60 000 quasar spectra of the SDSS-III/BOSS DR9 [5, 6] on the basis of their high quality, high signal-to-noise ratio and good spectral resolution ($< 85\,\mathrm{km\ s^{-1}}$ on average over a quasar forest). We use 12 redshift bins, spanning the range $2.1 < z < 4.5$, as shown on Fig. 1. We do the analysis on 420 Lyα data points, consisting of 12 redshift bins and 35 k bins.

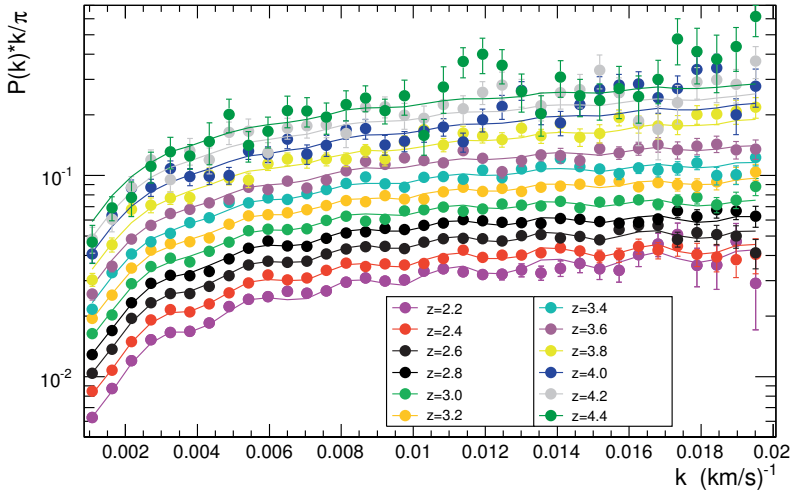

Figure 1 – *1D Lyα forest power spectrum from the SDSS-III/BOSS DR9 data. The solid curves show the best-fit model when considering Lyα data alone. The oscillations arise from Lyα-Si III correlations, which occur at a wavelength separation $\Delta\lambda = 9.2\AA$.*

The cosmic microwave background (CMB) data and results we use, are described in the 2015 Planck cosmological parameters paper [4]. In our analysis [7], we consider several subsets of Planck data and we obtain very similar results for the different configurations. Therefore, in this proceeding, we focus on the base configuration, denoted 'TT+lowP' as in [4] which uses the TT spectra at low and high multipoles and the polarization information up to multipoles $\ell = 29$ ('lowP').

The cosmological interpretation of the Lyα power spectrum measurement is obtained by comparison to a set of full hydrodynamical cosmological simulations that were produced specifically for that purpose (see Fig. 2). The methodology and technical framework for these simulations are presented in [2], while all issues concerning the inclusion of neutrinos in the pipeline and their impact on the power spectrum are described in detail in [3]. The neutrinos, considered as three degenerate species, are globally introduced as a third particle type, in addition to cold dark matter and baryons. The simulations were run using `CAMB` to compute the transfer functions and linear power spectra at $z = 30$, then `2LPT` (second-order Lagrangian Perturbation Theory) to compute the initial displacement of the particles, and finally `GADGET-3` [8] for the hydrodynamical processing. Using a splicing technique [2], we infer the flux power spectrum of an equivalent ($L = 100\,h^{-1}$ Mpc, $N = 3072$) simulation from a combination of three lesser ones: a scaled-down (25, 768) to provide high resolution on small scales, a large-box low-resolution (100, 768) for large scales, and a small-box low-resolution (25, 192) which bridges the preceding two at intermediate scales.

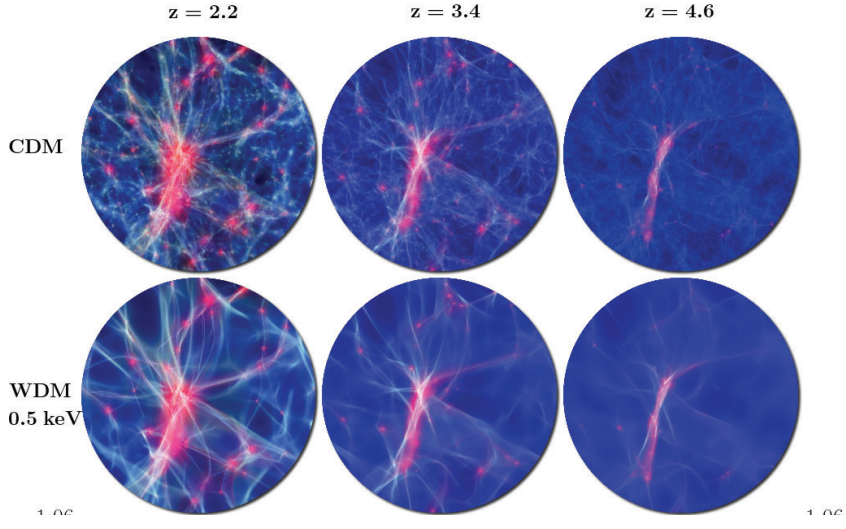

Figure 2 – *Visual inspection of the baryon gas density and temperature (encoded in intensity and color respectively), at $z = 2.5$, at $z = 3.4$ and at $z = 4.6$ for CDM (top panels) and for DM particle masses of 0.5 keV (bottom panels). Panels are 8 h^{-1}* Mpc *across in comoving coordinates.*

The ΛWDM analysis described in [9] shares a similar strategy. We just use two particle types, baryons and dark matter instead of three types. We explore two pure ΛWDM models with $m_X = 2.5$ and 5 keV thermal relics implemented using the neutrino mass degeneracy parameters in CAMB to encode $\Delta N_{\rm eff} \propto (T/T_\nu)^4$, which models the impact of any massive particle with temperature T coupled to photons prior to standard neutrino decoupling.

By varying the input parameters (cosmological and astrophysical parameters, total neutrino mass or inverse of thermal relic mass) around a central model chosen to be in agreement with the latest Planck results [4], the simulations were used to derive a second-order Taylor expansion,

including cross-terms, around the central model. Finally, we minimize a likelihood built around three categories of parameters which are floated. The first category describes the cosmological model assuming a flat Universe. The second category models the astrophysics within the IGM, and the relationship between the gas temperature and its density. The purpose of the third category (nuisance parameters) is to describe the imperfections of our measurement of the 1D power spectrum. This likelihood allows us to compare the measurement to the power spectrum predicted from the hydrodynamical simulations described above.

3 Results for ΛCDMν

The maximization of the likelihood with the Lyα data, imposing a Gaussian constraint $H_0 = 67.4 \pm 1.4$ gives a best-fit value of $\sum m_\nu$, the sum of the neutrino masses equal to 0.41 eV and compatible with 0 at about 1σ as described in[7]. The upper bound on $\sum m_\nu$ is thus 1.1 eV (95% C.L.). The cosmological parameters $\sigma_8 = 0.830 \pm 0.032$ and $\Omega_m = 0.293 \pm 0.013$ are in excellent agreement with the values derived independently from CMB data [4]. We observe a weak tension at the 2.3 σ level on the scalar index, $n_s = 0.939 \pm 0.010$. The fitted values of the astrophysical and nuisance parameters are all well within the expected range. The 2D constraints in the $n_s - \sigma_8$, $\sum m_\nu - \Omega_m$ and $\sum m_\nu - \sigma_8$ planes are shown as the red contours in Fig. 3. The neutrino mass is correlated to σ_8 (-48%), n_s (48%) and Ω_m (52%). Correlations between all other cosmological parameters have smaller amplitudes.

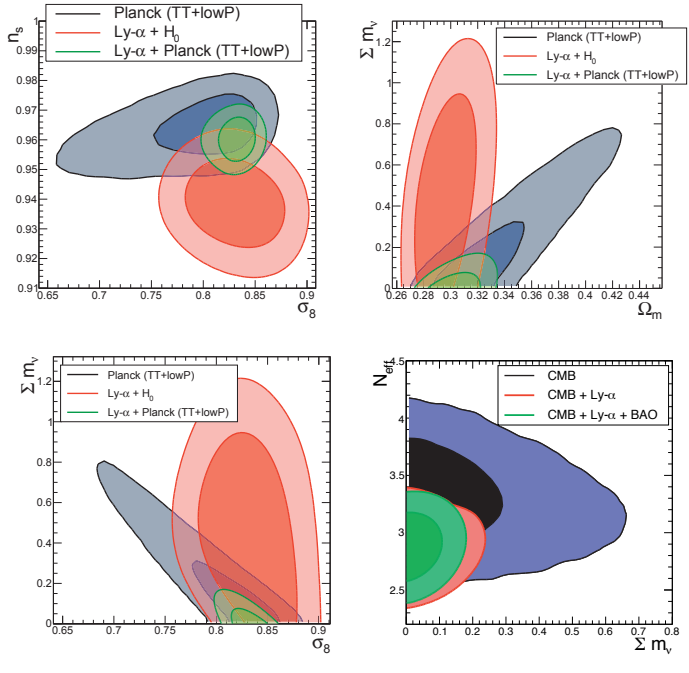

Figure 3 – **Unclockwise from top left:** *2D confidence level contours for the* $(\Omega_m, \sum m_\nu)$, (σ_8, n_s) *and* $(\sigma_8, \sum m_\nu)$ *cosmological parameters (see full description in [7]). The 68% and 95% confidence contours are obtained for the BOSS Ly*α *data with a Gaussian constraint* $H_0 = 67.4 \pm 1.4$ km s^{-1} Mpc^{-1}*, for the Planck 2015 data (TT+lowP) and for the combination of BOSS Ly*α *and Planck 2015.* **Bottom left** *2D confidence level contours for the* $(\sum m_\nu, N_{eff})$ *cosmological parameters for the CMB (Planck 2013, ACT, SPT and WMAP polarization) alone, then adding BOSS Ly*α *and finally BAO (see full description in [10]).*

Then we combine the Lyα likelihood (imposing no constraint on H_0) with the likelihood of Planck 2015 data. We constrain $\sum m_\nu$ to be less than 0.12 eV (at 95% C.L.) from Lyα and Planck TT+lowP, closer to to the inverted-hierarchy lower bound of 0.10 eV than current CMB-based limits. For comparison, Planck (TT+lowP) alone constrains the sum of the neutrino masses to $\sum m_\nu < 0.72\ eV$ and Planck (TT+lowP) with BAO measurements to $\sum m_\nu < 0.21$ eV.

In addition, with Ly-α data we can constrain the effective number of neutrino species, $N_{\rm eff}$, as described in a similar analysis [10]. Fig. 3-bottom-left summarizes the main results of our fitting procedure for the values of $N_{\rm eff}$ and $\sum m_\nu$, derived by combining CMB (Planck 2013 + ACT + SPT + WMAP polarization as defined in [11], blue contours) with Lyα forest data (red contours), or by further adding BAO information (green contours). Specifically, we obtain $N_{\rm eff} = 2.91^{+0.21}_{-0.22}$ (95% CL) and $\sum m_\nu < 0.15$ eV (95% C.L.) in the first case, and $N_{\rm eff} = 2.88 \pm 0.20$ (95% C.L.) and $\sum m_\nu < 0.14$ eV (95% C.L.) in the second. These tight constraints on $N_{\rm eff}$ exclude the possibility of a sterile neutrino thermalized with active neutrinos – or more generally of any decoupled relativistic relic with $\Delta N_{\rm eff} \simeq 1$ - at significance of over 5 σ, implying that there is no need for exotic neutrino physics in the concordance ΛCDM model. These results are fully consistent with the latest constraints reported by Planck 2015 [4].

4 Results for ΛCDMν with n_s running

The small tension between the values of n_s preferred by Lyα or Planck data motivates a combined fit allowing n_s to vary with scale. We thus introduce $\mathrm{d}n_s/\mathrm{d}\ln k$ by using the corresponding Planck chains and adapting the Lyα likelihood to include a running of n_s (see details in [7]). We choose a pivot scale $k_0 = 0.05\ \mathrm{Mpc}^{-1}$, the same as in the analyses led by the Planck collaboration in order to allow direct comparisons. The scalar mode power spectrum is then parameterized by a power law with

$$P_s = \left(\frac{k}{k_0}\right)^{n_s - 1 + \frac{1}{2}\mathrm{d}n_s/\mathrm{d}\ln k \ln(k/k_0)} . \quad (1)$$

The pivot scale k_0 is approximately in the middle of the logarithmic range of the scales probed by Planck. The Lyα forests cover scales ranging from $\sim 0.07\ \mathrm{Mpc}^{-1}$ to $\sim 1.7\ \mathrm{Mpc}^{-1}$, with a pivot near $k_{Ly\alpha} \sim 0.7\ \mathrm{Mpc}^{-1}$. The constraint that we can derive on the running index $\mathrm{d}n_s/\mathrm{d}\ln k$ comes mostly from the different levels of the power spectra at the CMB and Lyα pivot scales k_0 and $k_{Ly\alpha}$.

On the theoretical side, the simplest inflationary models predict that the running of the spectral index should be of second order in inflationary slow-roll parameters and therefore small, $|\mathrm{d}n_s/\mathrm{d}\ln k| \sim (n_s - 1)^2 \sim 10^{-3}$ [12]. Nevertheless, it is possible to accommodate a larger scale dependence of n_s, by adjusting the third derivative in the inflaton potential, for instance. On the experimental side, recent CMB experiments have a mixed history of null-results and a-few-sigma detections of running of the scalar index. The final 9-year WMAP analysis found no evidence of running using WMAP alone, with $\mathrm{d}n_s/\mathrm{d}\ln k = -0.019 \pm 0.025$ at 68% CL, while the combination of WMAP data with the first data releases from ACT and SPT found a negative running at nearly the 2σ level with $\mathrm{d}n_s/\mathrm{d}\ln k = -0.022 \pm 0.012$ [13]. The Planck 2015 results, while roughly consistent with zero running of the scalar spectral index, indicate a $\sim 1\sigma$ preference for negative running, $\mathrm{d}n_s/\mathrm{d}\ln k = -0.0084 \pm 0.0082$.

Allowing a running of n_s improves the fit χ^2 by ~ 10 compared to the results obtained for the same set of data but without running and it gives $n_s = 0.960 \pm 0.004$ at CMB pivot, k_0 and $\mathrm{d}n_s/\mathrm{d}\ln k = -0.0149^{+0.0050}_{-0.0048}$. This is driven by the fact that a negative running of order 10^{-2} is favored both by Planck data alone, and by the tension on n_s between Planck and Lyα data sets. The corresponding 2D contours are illustrated in figure 4, left plot.

As the global χ^2 is clearly improved by letting $\mathrm{d}n_s/\mathrm{d}\ln k$ free, it is interesting to study the impact of this extra parameter on the determination of $\sum m_\nu$ in the base ΛCDMν model with running. As shown on the right plot of the figure 4, the correlation between $\mathrm{d}n_s/\mathrm{d}\ln k$ and

$\sum m_\nu$ is small. By adding this free parameter, $\mathrm{d}n_s/\mathrm{d}\ln k$ we obtain a limit $\sum m_\nu < 0.19$ eV (95% C.L.) which is less constraining limit as expected. However, if we add the BAO data, we recover the constraint without the additional free parameter, $\sum m_\nu < 0.12$ eV (95% C.L.).

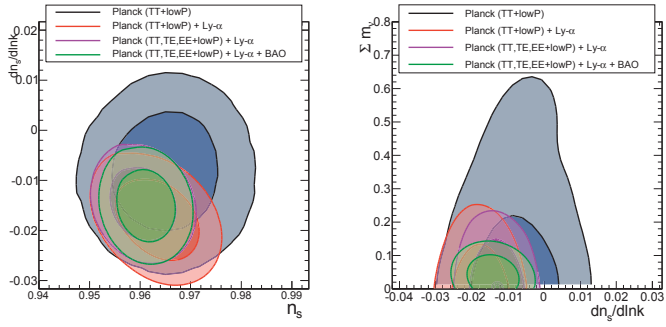

Figure 4 – *Constraints on the scalar spectral index n_s, the running $\mathrm{d}n_s/\mathrm{d}\ln k$, and $\sum m_\nu$. 68% and 95% confidence contours obtained for four combinations – Planck 2015 TT+lowP data alone, then adding BOSS Lyα, high-ℓ polarization from Planck (TE and EE) and finally BAO data.*

5 Results for ΛWDM cosmology

The likelihood used in the case of ΛWDM cosmology is quite similar to the likelihood described in the Sec. 3. The analysis is fully detailed in in [9]. Combining the Ly-α forest data with the expansion rate value of $H_0 = 67.3 \pm 1.0$ km s^{-1} Mpc^{-1} issued by the Planck 2015 [4], we obtain the most stringent lower limit on WDM mass to date, set at $m_X > 4.35$ keV for thermal relics.

Our work distinguishes itself from those of our predecessors [14, 15, 16] in a sharpened understanding of the systematics related to our numerical simulations and in the usage of a significantly larger sample of medium-resolution quasar spectra (SDSS-III) than previously (SDSS-I). Our QSO sample includes over four times as many medium-resolution spectra than previous SDSS studies, with all spectra selected for their high signal-to-noise ratio and good quality, and overall it includes more objects in the highest redshift bins. As the damping of small-scale perturbations due to free-streaming is more prominent at higher redshifts, the bounds on WDM particle mass are better constrained at higher redshifts. For instance, dropping the two highest redshift bins from our sample issues $m_X > 3.1$ keV, which is illustrative of their significance.

Finally, to obtain a constraint on the sterile neutrino mass, we consider a non resonantly production in which no lepton asymmetry is required. Using the Dodelson-Widrow [17] mechanism, in which the sterile neutrinos are produced by oscillations with the active neutrinos in a seesaw mechanism in the early Universe ($T \sim 100$ MeV for keV masses), we can derive a limit on non-resonantly-produced sterile neutrinos $m_s \gtrsim 26.4$ keV (95% C.L.). as shown on Fig. 5.

The work described in [9] focuses on early decoupled thermal relics (such as gravitinos for instance) and neutrinos produced in a Dodelson-Widrow mechanism, and allows us to set the strongest bounds on their mass. Other models with resonantly-produced sterile neutrino[16, 18] (which have been recently suggested as a plausible origin of the 3.55 keV line observed in the X-ray spectrum of galaxy clusters [19, 20]), will be investigated in a forthcoming study.

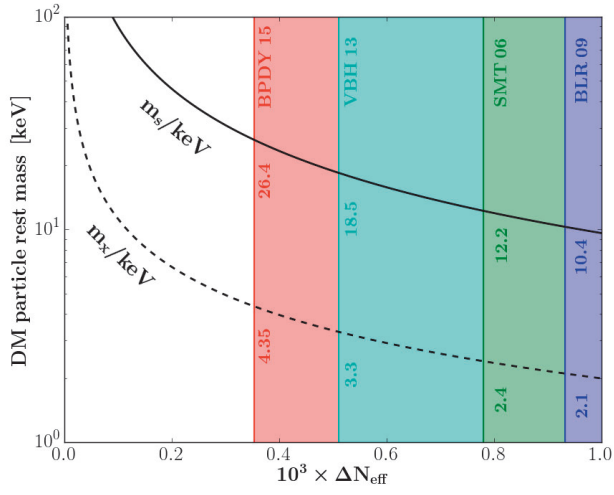

Figure 5 – Relation between $\Delta N_{\rm eff} \propto (T/T_\nu)^4$ and dark matter particle mass in the thermal relic (dotted line) and Dodelson-Widrow [17] sterile neutrino (solid line) cases. The dark matter lower-bound mass obtained by our analysis [9], labelled 'BPDY15' and previous works are illustrated by the solid black vertical lines: BLR09 [16], SMT06 [15] and VBH08 [14].

Acknowledgments

This work was done in collaboration with Nathalie Palanque-Delabrouille and Julien Baur. The author thanks Julien Lesgourgues, Graziano Rossi and Matteo Viel for their precious feedback and input, as well as Volker Springel for making `GADGET-3` available to our team. He acknowledges PRACE (Partnership for Advanced Computing in Europe) for awarding us access to resource curie-thin and curie-xlarge nodes based in France at TGCC, under allocation numbers 2010PA2777, 2014102371 and 2012071264.

References

[1] Palanque-Delabrouille, N., C. Yèche, A. Borde, et al. The one-dimensional Ly-alpha forest power spectrum from BOSS. *A. & A.*, 559:A85, 2013. `arXiv:1306.5896`.

[2] Borde, A., N. Palanque-Delabrouille, G. Rossi, et al. New approach for precise computation of Lyman-α forest power spectrum with hydrodynamical simulations. *JCAP*, 7:005, 2014. `arXiv:1401.6472`.

[3] Rossi, G., N. Palanque-Delabrouille, A. Borde, et al. Suite of hydrodynamical simulations for the Lyman-α forest with massive neutrinos. *A & A*, 567:A79, 2014. `arXiv:1401.6464`.

[4] Planck Collaboration, P. A. R. Ade, N. Aghanim, et al. Planck 2015 results. XIII. Cosmological parameters. *ArXiv:1502.01589*, 2015. `arXiv:1502.01589`.

[5] Ahn, C. P., R. Alexandroff, C. Allende Prieto, et al. The Ninth Data Release of the Sloan Digital Sky Survey: First Spectroscopic Data from the SDSS-III Baryon Oscillation Spectroscopic Survey. *ApJS*, 203:21, 2012. `arXiv:1207.7137`.

[6] Dawson, K. S., D. J. Schlegel, C. P. Ahn, et al. The Baryon Oscillation Spectroscopic Survey of SDSS-III. *The Astronomical Journal*, 145:10, 2013. arXiv:1208.0022.

[7] Palanque-Delabrouille, N., C. Yèche, J. Baur, et al. Neutrino masses and cosmology with Lyman-alpha forest power spectrum. *JCAP*, 11:011, 2015. arXiv:1506.05976.

[8] Springel, V., N. Yoshida, and S. D. White. GADGET: a code for collisionless and gasdynamical cosmological simulations. *New Astronomy*, 6:79–117, 2001. arXiv:astro-ph/0003162.

[9] Baur, J., N. Palanque-Delabrouille, C. Yèche, et al. Lyman-alpha Forests cool Warm Dark Matter. *ArXiv:1512.01981*, 2015. arXiv:1512.01981.

[10] Rossi, G., C. Yèche, N. Palanque-Delabrouille, et al. Constraints on dark radiation from cosmological probes. *Phys. Rev. D*, 92:063505, 2015. arXiv:1412.6763.

[11] Planck Collaboration, P. A. R. Ade, N. Aghanim, et al. Planck 2013 results. XVI. Cosmological parameters. 2013. arXiv:1303.5076.

[12] Kosowsky, A. and M. S. Turner. CBR anisotropy and the running of the scalar spectral index. *Phys. Rev. D*, 52:1739, 1995. astro-ph/9504071.

[13] Hinshaw, G., D. Larson, E. Komatsu, et al. Nine-year Wilkinson Microwave Anisotropy Probe (WMAP) Observations: Cosmological Parameter Results. *The Astrophysical Journal Supplement Series*, 208:19, 2013. arXiv:astro-ph.CO/1212.5226.

[14] Viel, M., G. D. Becker, J. S. Bolton, et al. How Cold Is Cold Dark Matter? Small-Scales Constraints from the Flux Power Spectrum of the High-Redshift Lyman-α Forest. *Phys. Rev. Lett.*, 100:041304, 2008. arXiv:0709.0131.

[15] Seljak, U., A. Makarov, P. McDonald, et al. Can Sterile Neutrinos Be the Dark Matter? *Phys. Rev. Lett.*, 97:191303, 2006. astro-ph/0602430.

[16] Boyarsky, A., J. Lesgourgues, O. Ruchayskiy, et al. Lyman-α constraints on warm and on warm-plus-cold dark matter models. *JCAP*, 5:12, 2009. arXiv:0812.0010.

[17] Dodelson, S. and L. M. Widrow. Sterile neutrinos as dark matter. *Phys. Rev. Lett.*, 72: 17–20, 1994. hep-ph/9303287.

[18] Boyarsky, A., J. Lesgourgues, O. Ruchayskiy, et al. Realistic Sterile Neutrino Dark Matter with KeV Mass does not Contradict Cosmological Bounds. *Physical Review Letters*, 102: 201304, 2009. arXiv:hep-ph/0812.3256.

[19] Bulbul, E., M. Markevitch, A. Foster, et al. Detection of an Unidentified Emission Line in the Stacked X-Ray Spectrum of Galaxy Clusters. *ApJ*, 789:13, 2014. arXiv:1402.2301.

[20] Boyarsky, A., O. Ruchayskiy, D. Iakubovskyi, et al. Unidentified Line in X-Ray Spectra of the Andromeda Galaxy and Perseus Galaxy Cluster. *Physical Review Letters*, 113:251301, 2014. arXiv:1402.4119.